

## **NONLINEAR DEFORMATION OF THIN ISOTROPIC AND ORTHOTROPIC SHELLS OF REVOLUTION WITH REINFORCED HOLES AND RIGID INCLUSIONS**

**V. A. Maksimyuk,\* E. A. Storozhuk,\* and I. S. Chernyshenko\*\***

**The stress–strain state of thin spherical, conical, and ellipsoidal shells made of nonlinear elastic orthotropic composites is analyzed numerically. The methods of successive approximations, the finite-difference method, and an original algorithm for the numerical discretization of a plane curve are used. The effect of the orthotropy and nonlinearity of composite materials, the geometry of shells, and the stiffness of the reinforcement (rings, inclusions) on the stress–strain state is studied**

**Keywords:** nonlinear elastic orthotropic composite, thin ellipsoidal shell, rigid inclusion, circular hole, finite-difference method

**Introduction.** Thin structural members such as plates and shells are often weakened with natural or artificial holes or rigid inclusions of various shapes. Artificial holes in shell members of structures subject to internal pressure are commonly reinforced with rods for further connection or closing by a rigid plug. This causes the redistribution of the stresses around the holes. Such a situation occurs near rigid inclusions in thin-walled structural members.

The stress concentration around rigid inclusions in isotropic elastoplastic and elastic shells is addressed in many studies such as [4–8, 15, 16]. Noteworthy are the two papers [13, 14] that generalize and develop studies on, in particular, the stress concentration in isotropic spherical shells with rigid inclusions.

Numerical results on the stress–strain state (SSS) of orthotropic shells made of nonlinear elastic composite materials (CMs) are summarized in [2, 12]. Spherical and ellipsoidal shells with a reinforced hole were considered in [1] and [10], respectively. A rigid inclusion as a limiting case of reinforcement of a hole with a rod of high stiffness was considered in [1]. Also, of interest is to study the nonlinear deformation of orthotropic shells of revolution with reinforcements, including a rigid inclusion.

In what follows, we will discuss results on the SSS of equiwide spherical, conical, and ellipsoidal shells (with widely varying ellipticity).

**1. Problem Statement. Methodical Aspects of Problem Solving.** Let us consider deep shells made of orthotropic nonlinear elastic CMs [2] undergoing nonlinear deformation under surface loads and boundary forces and moments (Fig. 1). Let the effective mechanical characteristics and nonlinear properties of the orthotropic composite be known, and its axes of orthotropy be aligned with the line-of-curvature coordinate axes ( $s, \theta, \gamma$ ) on the mid-surface of the shell.

Under certain levels of load, the anisotropic material of the shell manifests nonlinear properties, the strains being small. This allows us to use the geometrically linear theory of shells [2] and the theory of anisotropic plasticity [3] to derive the basic equations.

Methodologically, the analysis of the SSS of irregularly shaped shells with a reinforced hole is complicated by the problem of joining components of different dimensionality. This problem is simpler if the deformation of shells of revolution is axisymmetric. Three types of boundary conditions can be prescribed on the surface of a shell with a rigid inclusion: (i) the portion of the shell's boundary to which the inclusion is attached is undeformable (deformation boundary conditions); (ii) the

---

S. P. Timoshenko Institute of Mechanics, National Academy of Sciences of Ukraine, 3 Nesterova St., Kyiv, Ukraine 03057, e-mail: \*desc@inmech.kiev.ua, \*\*prik1@inmech.kiev.ua. Translated from *Prikladnaya Mekhanika*, Vol. 49, No. 6, pp. 67–74, November–December 2013. Original article submitted December 28, 2011.

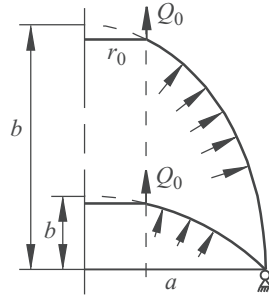


Fig. 1

displacement and angles of rotation on the shell's boundary are expressed in terms of the rigid-body displacement of the inclusion (geometrical boundary conditions); (iii) the boundary of the shell is reinforced with a ring of high stiffness; using such a thin curved element as a reinforcement is acceptable in shells of revolution.

If the hole is reinforced with a thin elastic element (ring) of given stiffness to which a shearing force  $Q_0$  is applied (Fig. 1), then we have the following boundary conditions at the interface ( $s = 0$ ) between the ring and the shell [1, 10]:

$$\begin{aligned}
 Q_s \sin \varphi + T_s \cos \varphi - \frac{F_0 E_0}{r_0^2} (w \sin \varphi + u \cos \varphi) &= 0, \\
 Q_s \cos \varphi - T_s \sin \varphi &= -Q_0, \\
 M_s + Q_s r_1 + T_s r_2 + \frac{J_0 E_0}{12 r_0^2} \vartheta &= 0,
 \end{aligned} \tag{1}$$

where  $T_s, Q_s, M_s$  are the internal forces and moment;  $w, u, \vartheta$  are the deflection, tangential displacement, and the angle of rotation of the normal around the tangent to the hole boundary;  $\varphi$  is the angle between the normal and the axis of revolution at the junction;  $r_0, r_1, r_2$  are the distance from the center of gravity of the ring to the axis of revolution and its displacements along the coordinate lines  $s$  and  $\gamma$ , respectively;  $E_0, F_0, J_0$  are the elastic modulus of the ring in the circumferential direction, its cross-sectional area, and the moment of inertia of its cross section.

For a ring of rectangular cross-section of height  $a_0$  and width  $b_0$ , we have

$$F_0 = a_0 b_0, \quad J_0 = a_0^3 b_0 / 12.$$

Let  $E_0$  of the rigid inclusion be very high. Then, the boundary conditions (1) reduce to the following limiting form:

$$\begin{aligned}
 w \sin \varphi + u \cos \varphi &= 0, \\
 Q_s \cos \varphi - T_s \sin \varphi &= -Q_0, \\
 \vartheta &= 0,
 \end{aligned} \tag{2}$$

which represents the equilibrium of a perfectly rigid inclusion. The outer boundary ( $s = s_k$ ) of the shell is hinged

$$u = 0, \quad w = 0, \quad M_s = 0. \tag{3}$$

The nonlinear governing system of equations for displacements, including the equilibrium equations and the boundary conditions (1) or (2) and (3) can be solved numerically [12] using the method of successive approximations and the finite-difference method (FDM). For the purposes of the FDM, the meridian of the shell of revolution should be partitioned into arcs of given length. This problem cannot be solve analytically in the general case (including ellipsoidal shells). To solve these (non)linear problems, it is proposed to use the algorithm for the numerical discretization of a plane curve  $F(x, z) = 0$  [9] based on a Newton-type method.

TABLE 1

$N$	$\tilde{\gamma}$	LP		NP	
		$\sigma_s$	$\sigma_\theta$	$\sigma_s$	$\sigma_\theta$
1	0.5	10	2694	10	1788
	-0.5	10	1543	10	1437
2	0.5	900	1284	753	894
	-0.5	-701	787	-616	542
3	0.5	425	416	411	399
	-0.5	115	328	113	328
4	0.5	231	103	231	103
	-0.5	439	163	439	163
5	0.5	203	58	197	56
	-0.5	485	139	467	135

**2. Stress State of Shells of Revolution.** Let us consider a family of equiwide shells of revolution (spherical, conical, ellipsoidal) in which the distance from the inner ( $r=r_0, s=0$ ) and outer ( $r=r_k, s=s_k$ ) edges to the axis of revolution  $OZ$  does not change, while the shape and length of the meridian and the distance from the hole boundary to the equatorial plane along the axis are variable (Fig. 1). The meridian of such shells is described by the equation

$$F(x, z) = \left(\frac{x}{a}\right)^n + \left(\frac{z}{b}\right)^n - 1 = 0 \quad (n=1, 2). \quad (4)$$

Let the shells be subject to internal pressure  $p$  and shearing force  $Q_0 = pr_0 / 2$

**2.1. Spherical Shell.** Let us analyze the SSS around a circular hole of radius  $r_0 = 22.22h$  in thin spherical ( $n=2, a=b=R$  in (4)) orthotropic shells of radius  $R = 120h$  [10] whose outer edge is bounded by an equatorial plane ( $r_k = 120h, s_k = 165.19h$ ).

Let internal pressure ( $p = 5$  MPa) and shearing force  $Q_0$  be applied to the edge of the hole. The mechanical characteristics of the material (nonlinear elastic orthotropic eight-layer organic plastic [2]) of the shells:  $E_{ss} = 26.8$  GPa,  $E_{\theta\theta} = 46.5$  GPa,  $\nu_{\theta s} = 0.166$ ,  $q_{ss} = 4.32$ ,  $q_{\theta\theta} = 2$ ,  $q_{s\theta} = -0.64$ . The other quantities in Eqs. (1) and the function describing the anisotropic nonlinear properties of the material can be found in [2].

Let the hole be reinforced with a linear elastic ring of rectangular cross-section [10] of height  $a_0 = 20h$  and width  $b_0 = h$  with  $r_1 = r_2 = 0$  and  $E_0 = 46.5$  GPa, which corresponds to the third type of reinforcement. The other types ( $N$ ) are: (i) no reinforcement ( $E_0 = 0$ ), (ii) reinforcement of low stiffness ( $E_0 = 4.65$  GPa), (iv) reinforcement of higher stiffness ( $E_0 = 465$  GPa), (v) rigid inclusion ( $E_0 = 4.65 \cdot 10^9$  GPa).

Linear (LP) and nonlinear (NP) problem statements are considered. The meridian is partitioned into regular intervals by 321 nodal points. The difference between the maximum strains found in two subsequent approximations does not exceed  $10^{-3}$ .

Table 1 summarizes the values of the meridional ( $\sigma_s$ ) and circumferential ( $\sigma_\theta$ ) stresses (MPa) on the outer ( $\tilde{\gamma} = \gamma / h = 0.5$ ) and inner ( $\tilde{\gamma} = -0.5$ ) surfaces near the hole ( $s = 0$ ). It can be seen that the stresses are maximum on the boundary of the hole for

TABLE 2

$N$	$\tilde{\gamma}$	$\sigma_s$	$\sigma_\theta$
1	0.5	42	717
	-0.5	42	647
3	0.5	-19	56
	-0.5	176	114
5	0.5	-33	-26
	-0.5	263	75

TABLE 3

$N$	$\tilde{\gamma}$	LP		NP	
		$\sigma_s$	$\sigma_\theta$	$\sigma_s$	$\sigma_\theta$
5	0.5	502	787	470	741
	-0.5	220	707	235	742

all types of reinforcement. The hoop stresses on the outer surface are maximum for nonreinforced and weakly reinforced holes ( $N = 1, 2$ ), while the meridional stresses on the inner surface are maximum for the stiffer reinforcement ( $N = 4, 5$ ).

The third type of reinforcement is close to optimal when the maximum meridional and hoop stresses are equal. Noteworthy is the presence of compressive stresses when the hole is weakly reinforced ( $N = 2$ ). Physical nonlinearity manifests itself when the hole is not reinforced or reinforced with a ring of low stiffness. With increase in the stiffness, the reinforcement has either weak effect ( $N = 3$ ) or no effect ( $N = 4$ ). The influence of nonlinearity on the stress distribution is insignificant with a rigid inclusion.

**2.2. Conical Shell.** Let us analyze the SSS of a truncated conical ( $n = 1$ ,  $a = 120h$ ,  $b = 144.69h$  B (4),  $s_k = 153.16h$ ) orthotropic shell generated by revolving the chord connecting the ends of the meridian of the spherical shell considered above. Its mechanical characteristics are the same as those of the spherical shells.

Table 2 summarizes the values of the stresses (MPa) near the truncated portion of the cone found by solving the nonlinear problem. They are almost half those in the spherical shell. Physical nonlinearity is not manifested if there is a reinforcement or a rigid inclusion in the truncation zone ( $s = 0$ ). If there is no reinforcement ( $N = 1$ ), ignoring the nonlinear properties of the composite increases the stress from  $\sigma_\theta = 717$  MPa to  $\sigma_\theta = 763$  MPa.

Unlike the spherical shell, the maximum stresses (Table 3) in the conical shell are observed near the hinged edge in the section  $s = 0.9s_k$  and these are hoop stresses. In this section, they exceed approximately two times the stresses in the spherical shell where they are close to the membrane stresses. Note that Table 3 gives stresses only for the rigid inclusion because the reinforcement of the truncated edge of the cone has almost no effect on the SSS near the fixed edge.

**2.3. Ellipsoidal Shells.** Let us consider oblong ( $n = 2$ ,  $a = 120h$ ,  $b = 240h$  in (4),  $s_k = 266.03h$ ; Tables 4–6) and oblate ( $n = 2$ ,  $a = 120h$ ,  $b = 60h$  in (4),  $s_k = 122.6h$ ; Table 7) ellipsoidal shells. Their mechanical characteristics are the same as those of the spherical shell.

Table 4 presents the stress distribution along the boundary of the nonreinforced and weakly reinforced holes ( $N = 1, 2$ ) in the oblong shell found by solving the linear and nonlinear problems. Table 5 summarizes the results for the stiffer

TABLE 4

$N$	$\tilde{\gamma}$	LP		NP	
		$\sigma_s$	$\sigma_\theta$	$\sigma_s$	$\sigma_\theta$
1	0.5	20	1687	20	1284
	-0.5	20	1143	20	1063
2	0.5	546	773	498	661
	-0.5	-405	484	-388	423

TABLE 5

$N$	$\tilde{\gamma}$	$\sigma_s$	$\sigma_\theta$
3	0.5	192	210
	-0.5	109	188
4	0.5	68	38
	-0.5	284	100
5	0.5	51	14
	-0.5	308	88

TABLE 6

NP, LP	$\tilde{\gamma}$	$e_s \cdot 10$	$e_\theta \cdot 10$	$\sigma_s$	$\sigma_\theta$
NP	0.5	0.118	0.101	379	548
	-0.5	0.046	0.102	213	534
LP	0.5	0.112	0.097	393	566
	-0.5	0.045	0.098	206	515

reinforcement and the rigid inclusion obtained by solving only the nonlinear problem because nonlinearity in these cases is manifested near the hinged edge, but not on the boundary of the hole or the inclusion.

The deformation behavior of the oblong ellipsoidal shell is generally similar to that (see Sec. 2.1) of the spherical shell with the difference that the stresses on the hole boundary in the oblong shell are maximum only if the hole is not reinforced or weakly reinforced. In the other cases, the hoop stresses near the hinged edge in the section  $s = 0.95s_k$  are maximum, as in the conical shell (Sec. 3).

Table 6 shows how physical nonlinearity affects the SSS in the section  $s = 0.95s_k$  of the oblong shell with a rigid inclusion. It can be seen that nonlinearity has a stronger effect on the meridional strains ( $e_s$ ) than on the hoop stresses ( $\sigma_\theta$ ), which tend to  $pa/h = 600$  MPa due to the elongated shape of the shell along the axis of symmetry, as in the cylindrical shell.

TABLE 7

$N$	$\tilde{\gamma}$	LP		NP	
		$\sigma_s$	$\sigma_\theta$	$\sigma_s$	$\sigma_\theta$
1	0.5	5	4314	6	2582
	-0.5	5	2041	5	1988
2	0.5	1442	2132	1090	1178
	-0.5	-1130	13428	-837	765
3	0.5	875	811	740	613
	-0.5	138	599	249	635
4	0.5	602	246	592	234
	-0.5	722	281	718	266
5	0.5	560	161	565	165
	-0.5	811	233	766	228

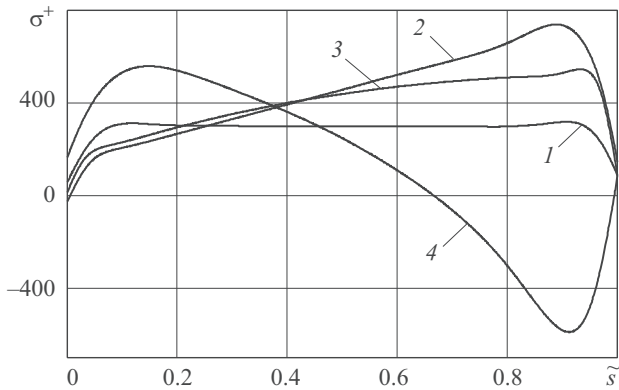


Fig. 2

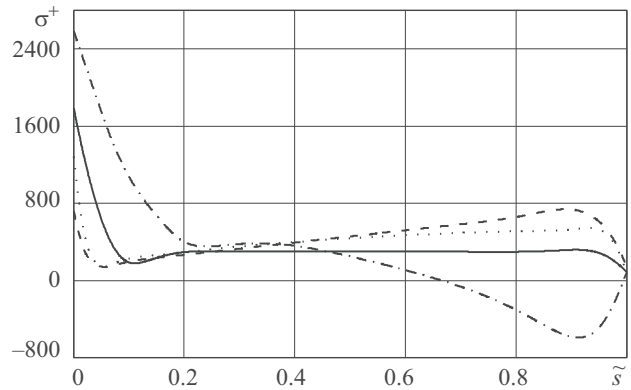


Fig. 3

The stresses in the oblate shell (Table 7) exceed the stresses in all the shells considered above. The deformation behavior of the oblate ellipsoidal shell is to a lesser degree similar to that (Sec. 2.1) of the spherical shell compared with the oblong shell. A distinguishing feature of the oblate shell is the presence of a zone of compressive hoop stresses near the outer edge (curve 4 in Fig. 2).

Figure 2 show the variation of the hoop stresses ( $\sigma^+$ , MPa) along the meridian ( $\tilde{s} = s/s_k$ ) on the outside surfaces of shells with the rigid inclusion. Curves 1, 2, 3, 4 represent the spherical, conical, and oblong and oblate ellipsoidal shells, respectively.

For comparison, Fig. 3 shows similar curves for the spherical (solid line), conical (dashed line), oblong (dotted line) and oblate (dash-and-dot line) ellipsoidal shells with a free hole.

**3. Effect of Orthotropy on the Stress State of Spherical Shells.** By changing the orientation of the axes of orthotropy of composites relative to the coordinate axes, we can analyze its effect on the SSS of the shell, the other conditions being given.

TABLE 8

$\tilde{E}$	$p$ , MPa	$\tilde{\gamma}$	LP		NP	
			$\sigma_s / p$	$\sigma_\theta / p$	$\sigma_s / p$	$\sigma_\theta / p$
0.576	5	0.5	40.6	11.6	39.4	11.2
		-0.5	97.6	27.8	93.4	27
1.735	5	0.5	-30.8	-5	-35	-5.8
		-0.5	187	31	170	27.6
1.000	3	0.5	16.3	5	-4.3	-1.3
		-0.5	126	40.3	85.3	40

TABLE 9

$\tilde{E}$	$p$ , MPa	$\tilde{\gamma}$	LP	NP
			$\sigma_\theta / p$	$\sigma_\theta / p$
0.576	5	0.5	539	358
		-0.5	309	287
1.735	5	0.5	402	254
		-0.5	282	225
1.000	1	0.5	464	248
		-0.5	296	223

Let us compare the SSS of a spherical shell (Sec. 2) with  $\tilde{E} = E_{ss} / E_{\theta\theta} = 0.576$  to the SSS of the same shell with the orientation of the axes of orthotropy changed so that  $\tilde{E} = 1.735$  and to the SSS of an isotropic elastoplastic shell made of aluminum alloy with the following characteristics [7, 8]:  $E_{ss} = E_{\theta\theta} = E = 67$  GPa,  $\nu = 0.3 \dots 0.5$ ,  $\sigma_n = 130$  MPa,  $\varepsilon_n = 0.002$ .

For the shells with a rigid inclusion, the comparison is made in Table 8. It can be seen that in the nonlinear case, orthotropy is manifested to a lesser degree than in the linear case. In the linear case, the magnitude of the stresses in the isotropic shell is between those of the stresses in the orthotropic shells. Nonlinearity in the isotropic shell affects the SSS under lower loads. Increasing the elastic modulus in the meridional direction increases the stresses on the hole boundary, which is due to the stronger interaction between the stiffer portion of the shell near the rigid inclusion and the less stiff middle portion of the shell.

For comparison, Table 9 presents similar data for a spherical shell with a free (nonreinforced) hole. It can be seen that in the nonlinear case, orthotropy is manifested to a greater degree than in the linear case. Increasing the elastic modulus in the meridional direction also decreases the stresses on the hole boundary, which is due to the stronger reinforcing effect of the major portion of the shell on its free edge.

**Conclusions.** The deformation behavior of oblong and oblate ellipsoidal shells is essentially different. The oblong ellipsoidal shell behaves as a conical shell. The oblate shell has a compression zone near the hinged edge.

Increasing the stiffness of the reinforcement of the hole leads to nonmonotonic redistribution of the stresses on its boundary. The maximum stresses on the hole boundary first decrease, becoming almost equal when reinforcement is optimal, and then increase.

The effect of orthotropy on the SSS around the hole depends on the stiffness of the reinforcement and is opposite in two limiting cases: free hole and rigid inclusion.

## REFERENCES

1. V. P. Georgievskii, V. A. Maksimyuk, and I. S. Chernyshenko, "Reinforcement of the edge of a hole in orthotropic physically nonlinear shells of revolution," *Prikl. Mekh.*, **23**, No. 6, 125–127 (1987).
2. A. N. Guz, A. S. Kosmodamianskii, V. P. Shevchenko, et al., *Stress Concentration*, Vol. 7 of the 12-volume series *Mechanics of Composite Materials* [in Russian], A.S.K., Kyiv (1998).
3. V. A. Lomakin, "On the theory of anisotropic plasticity," *Vestn. MGU, Ser. Mat. Mekh.*, No. 4, 49–53 (1964).
4. Yu. S. Solomonov, V. P. Georgievskii, A. Ya. Nedbai, and V. A. Andryushin, *Methods for the Design of Cylindrical Shells Made of Composite Materials* [in Russian], Fizmatlit, Moscow (2009).
5. D. H. Bonde and K. P. Rao, "Thermal stresses in a cylindrical shell containing a circular hole or a rigid inclusion," *Nucl. Eng. Design*, **40**, No. 2, 337–346 (1977).
6. V. N. Chekhov and S. V. Zakora, "Stress concentration in a transversely isotropic spherical shell with two circular rigid inclusions," *Int. Appl. Mech.*, **47**, No. 4, 441–448 (2011).
7. I. S. Chernyshenko, "Elastic-plastic state of shells of revolution with a rigid circular inclusion," *Int. Appl. Mech.*, **16**, No. 2, 130–134 (1980).
8. I. S. Chernyshenko, "Nonlinear deformation of isotropic and orthotropic shells with holes reinforced by a rigid elastic element," *Int. Appl. Mech.*, **25**, No. 1, 54–59 (1989).
9. I. S. Chernyshenko and V. A. Maksimyuk, "On the stress–strain state of toroidal shells of elliptical cross section formed from nonlinear elastic orthotropic materials," *Int. Appl. Mech.*, **36**, No. 1, 90–97 (2000).
10. V. P. Georgievskii, A. N. Guz, V. A. Maksimyuk, and I. S. Chernyshenko, "Numerical analysis of the nonlinearly elastic state around cutouts in orthotropic ellipsoidal shells," *Int. Appl. Mech.*, **25**, No. 12, 1207–1212 (1989).
11. A. N. Guz, E. A. Storozhuk, and I. S. Chernyshenko, "Nonlinear two-dimensional static problems for thin shells with reinforced curvilinear holes," *Int. Appl. Mech.*, **45**, No. 12, 1269–1300 (2009).
12. V. A. Maksimyuk, E. A. Storozhuk, and I. S. Chernyshenko, "Using mesh-based methods to solve nonlinear problems of statics for thin shells," *Int. Appl. Mech.*, **45**, No. 1, 32–56 (2009).
13. E. Reissner and F. Y. M. Wan, "Further considerations of stress concentration problems for twisted or sheared shallow spherical shells," *Int. J. Solids Struct.*, **31**, No. 16, 2153–2165 (1994).
14. E. Reissner and F. Y. M. Wan, "Static-geometric duality and stress concentration in twisted and sheared shallow spherical shells," *Comp. Mech.*, **22**, 437–442 (1999).
15. V. P. Shevchenko and S. V. Zakora, "On the mutual influence of closely located circular holes with rigid contours in a spherical shell," *J. Math. Sci.*, **174**, No. 3, 322–330 (2011).
16. S. V. Zakora and Val. N. Chekhov, "Stress state of a transversely isotropic spherical shell with a rigid circular inclusion," *Int. Appl. Mech.*, **41**, No. 12, 1384–1390 (2005).